

Operator Growth in Open Quantum Systems

Thomas Schuster^{1,2} and Norman Y. Yao³¹Department of Physics, University of California, Berkeley, California 94720, USA²Walter Burke Institute for Theoretical Physics and Institute for Quantum Information and Matter, California Institute of Technology, Pasadena, California 91125, USA³Department of Physics, Harvard University, Cambridge, Massachusetts 02138, USA

(Received 28 October 2022; accepted 6 September 2023; published 18 October 2023)

The spreading of quantum information in closed systems, often termed scrambling, is a hallmark of many-body quantum dynamics. In open systems, scrambling competes with noise, errors, and decoherence. Here, we provide a universal framework that describes the scrambling of quantum information in open systems: we predict that the effect of open-system dynamics is fundamentally controlled by operator size distributions and independent of the microscopic error mechanism. This framework allows us to demonstrate that open quantum systems exhibit universal classes of information dynamics that fundamentally differ from their unitary counterparts. Implications for the Loschmidt echo, nuclear magnetic resonance experiments, and the classical simulability of open quantum dynamics will be discussed.

DOI: 10.1103/PhysRevLett.131.160402

Introduction.—Conventionally, the study of quantum many-body systems has focused on the prediction of few-body observables, such as local correlation functions. More recently, sparked by fundamental questions in quantum thermalization and chaos [1], the classical simulation of quantum systems [2], and quantum gravity [3], physicists have turned to a complementary pursuit: quantifying the complexity of many-body *dynamics* itself.

At the heart of this pursuit is the notion of quantum information *scrambling*; across nearly the entirety of interacting many-body quantum systems, information encoded in initially local operators grows to become highly nonlocal [4–6]. Remarkably, recent experimental advances have enabled the direct measurement of scrambling—a task that, most commonly, utilizes backwards time evolution [7–14], but can also be performed using multiple copies of the system [15–17] or randomized measurements [18,19]. In such systems, the interplay between scrambling dynamics, extrinsic decoherence, and experimental noise motivates an essential question: What is the nature of quantum information scrambling in *open* quantum systems [13,16,20–31]?

In this Letter, we introduce a universal framework—based upon *operator size distributions* [32–35]—for capturing the effect of local errors on scrambling dynamics. In particular, we conjecture that the propagation of errors in chaotic many-body systems is fundamentally controlled by the size distributions of time-evolved operators and independent of the microscopic error mechanism. Our framework immediately offers predictions for both the Loschmidt echo [36–38] and out-of-time-ordered correlation (OTOC) functions [39,40]. In particular, we predict that the decay of the Loschmidt echo, which measures the fidelity associated with backwards time evolution, occurs at

a rate proportional to the operator’s size. Meanwhile, we predict that the decay of the OTOC, which measures the growth of local operators, is inhibited by open-system dynamics (by an amount proportional to the width of the operator’s size distribution).

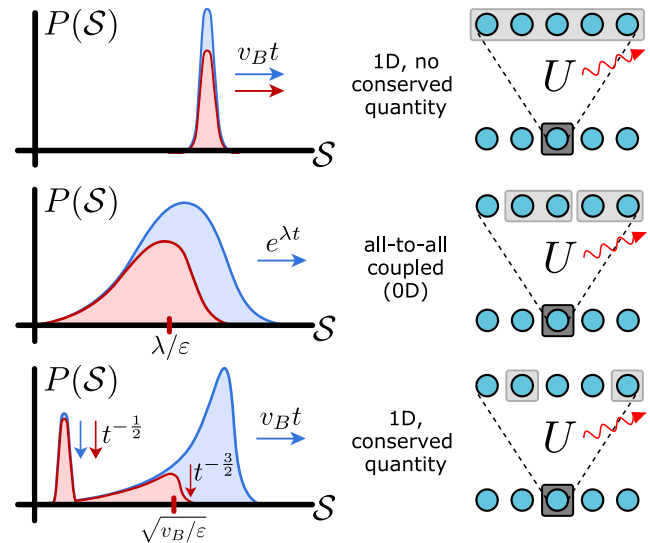


FIG. 1. Left: size distributions for three classes of systems under unitary (blue) versus open (red) dynamics. Rightward arrows denote growth in time to larger sizes, ticks denote a fixed size, and downward arrows denote loss of probability at a given size. Right: qualitative depiction of open-system operator growth. In all cases, operators lose normalization due to open dynamics (dark to light gray boxes). In the latter two classes, operators are dominated by smaller size components compared to unitary evolution (smaller boxes).

TABLE I. Operator growth under various dynamics.

System	Unitary dynamics	Open dynamics
$(d \geq 1)$ D, no conservation law	$\bar{\mathcal{S}} \sim t^d$ peaked $P(\mathcal{S})$	$\bar{\mathcal{S}} \sim t^d$ $\log(\mathcal{N}) \sim \epsilon t^{d+1}$
1D, conservation law	$\bar{\mathcal{S}} \sim t$ bimodal $P(\mathcal{S})$	$\bar{\mathcal{S}} \sim 1/\epsilon t$ $\mathcal{N} \sim 1/\sqrt{t}$
All-to-all coupled (0D)	$\bar{\mathcal{S}} \sim e^{\lambda t}$ broad $P(\mathcal{S})$	$\bar{\mathcal{S}} \sim \lambda/\epsilon$ $\log(\mathcal{N}) \sim \lambda t$
$(d \geq 1)$ 1D, long range	Superballistic broad $P(\mathcal{S})$	Ballistic $\log(\mathcal{N}) \sim \epsilon t^{d+1}$
Free fermion integrable	$\bar{\mathcal{S}} \sim t$ broad $P(\mathcal{S})$	$\bar{\mathcal{S}} \sim 1/\epsilon t$ $\mathcal{N} \sim 1/\epsilon t^2$

We leverage our framework to characterize operator growth in five distinct classes of open quantum systems, which vary in their dimensionality, range of interaction, conservation laws, and integrability (Table I, Figs. 1–3). In each class, our framework yields markedly distinct predictions for the Loschmidt echo and OTOCs. We hypothesize that these results provide a theoretical underpinning for recent nuclear magnetic resonance (NMR) experiments [9–11], and also serve to resolve apparent disagreements between previous empirical studies of open-system scrambling [13,24,25]. Finally, we propose and analyze a protocol for measuring operator size distributions via engineered dissipation.

Operator size distributions.—We begin with a simple example to build intuition. Consider a lattice of qubits acted on by a series of local quantum gates, each featuring some error ϵ , before measuring a local operator \hat{M} . Noting that the measurement can only be influenced by gates in its past light cone, a naive estimate of the measurement fidelity is $\mathcal{F} \approx (1 - \epsilon)^{\mathcal{V}_{\text{LC}}}$, where \mathcal{V}_{LC} is the light cone volume, i.e., the number of gates it contains [13,20]. This relation in fact already contains the essential intuition underlying our work: a connection between the measurement fidelity of a local operator and the operator’s growth under Heisenberg evolution. By generalizing the light cone volume using operator size distributions, we will show that this connection is significantly richer and more universal than the above example suggests [5,33].

To introduce the notion of an operator’s size distribution, we first define the size of a Pauli string, \hat{R} , as its number of nonidentity elements; for instance, $\hat{R} = Y \otimes \mathbb{1} \otimes Z \otimes X$ has size $\mathcal{S}_R = 3$. From this, one can define the size superoperator:

$$\mathcal{S}\{\hat{\mathcal{O}}\} \equiv -\sum_{\hat{P}_i} (\hat{P}_i \hat{\mathcal{O}} \hat{P}_i^\dagger - \hat{\mathcal{O}})/4, \quad (1)$$

which gives $\mathcal{S}\{\hat{R}\} = \mathcal{S}_R \hat{R}$, where $\hat{P}_i \in \{\hat{1}_i, \hat{X}_i, \hat{Y}_i, \hat{Z}_i\}$ are single-qubit Pauli operators [35]. More general operators can be expressed as a sum of Pauli strings, $\hat{\mathcal{O}} = \sum_{\hat{R}} c_R \hat{R}$, and thereby possess a *size distribution*, $P(\mathcal{S}) = \sum_{\{\mathcal{S}_R = \mathcal{S}\}} |c_R|^2$, with normalization $\mathcal{N} = \langle \hat{\mathcal{O}}^\dagger \hat{\mathcal{O}} \rangle = \sum_R |c_R|^2$; here, $\langle \cdot \rangle \equiv \text{Tr}(\cdot)/\text{Tr}(\mathbb{1})$ represents the infinite temperature expectation value. We note that the operator’s size distribution is closely related to out-of-time-ordered correlation functions, $\langle \hat{M}(t) \hat{P}_j \hat{M}(t) \hat{P}_j \rangle$. As the operator $\hat{M}(t)$ grows to have support on site j , the OTOC typically decays to zero. From Eq. (1), one immediately sees that the average size of $\hat{M}(t)$ is directly proportional to unity minus the OTOC averaged over all single-qubit Pauli operators:

$$\bar{\mathcal{S}} = \frac{\langle \hat{M}(t) \mathcal{S}\{\hat{M}(t)\} \rangle}{\langle \hat{M}(t) \hat{M}(t) \rangle} = \frac{1}{4} \sum_{\hat{P}_i} \left(1 - \frac{\langle \hat{M}(t) \hat{P}_i \hat{M}(t) \hat{P}_i \rangle}{\langle \hat{M}(t) \hat{M}(t) \rangle} \right). \quad (2)$$

Open-system operator growth hypothesis.—Let us now turn to open quantum systems. Operator evolution is typically governed by the Lindblad master equation:

$$\partial_t \hat{M} = i[\hat{H}, \hat{M}] - \sum_{\alpha} \epsilon_{\alpha} \left(\hat{L}_{\alpha}^\dagger \hat{M} \hat{L}_{\alpha} - \frac{1}{2} \{ \hat{L}_{\alpha}^\dagger \hat{L}_{\alpha}, \hat{M} \} \right). \quad (3)$$

The first term describes unitary time evolution, while the second describes a sum of local error processes, each characterized by a Lindblad operator, \hat{L}_{α} , and an associated error rate, ϵ_{α} .

Our central conjecture is that the effects of local errors on operator growth are in fact captured by a much simpler, effective Lindblad equation:

$$\partial_t \hat{M} = i[\hat{H}, \hat{M}] - \epsilon \mathcal{S}\{\hat{M}\}, \quad (4)$$

where \mathcal{S} is the size superoperator. This conjecture is rooted in the following intuition: larger size operators are affected by a greater number of local error processes, and thus decohere at a faster rate [41]. In effect, this model replaces the original Lindblad operators with isotropic decoherence at each qubit [Eq. (1)].

We expect Eq. (4) to apply to the large-size components of operators whenever the error rate is small compared to the unitary interaction strength, $\epsilon \ll J$, and the dynamics are ergodic. In these conditions, the large-size components of \hat{M} will involve exponentially many Pauli strings that vary rapidly in time compared to the error rate. We expect these properties to “average” the effect of Lindblad operators such that their action depends solely on whether they are in the support of a given component of \hat{M} , independent of their precise microscopic form. The number of Lindblad operators in the support is proportional to the size. We refer to the Supplemental Material for a detailed analytic discussion [44].

Finally, we conjecture that our framework also applies to an alternate scenario (often explored in NMR experiments [9–12]), where one evolves forward *unitarily* via a Hamiltonian, H , and backward via a perturbed Hamiltonian, $-H + \eta\delta H$ [54,55]. Naively, this scenario features perturbations that are highly correlated in time and space, and thus outside the Lindbladian framework. However, in ergodic many-body dynamics, one expects such correlations to quickly decay outside of some thermalization time (τ_{th}) and length (ξ_{th}). This assumption leads to a Fermi’s golden rule [55,56] estimate of an effective decoherence rate, $\varepsilon \sim \eta^2 \tau_{\text{th}} \xi_{\text{th}}$ [44].

Open-system scrambling dynamics.—Our framework predicts two effects of open-system dynamics on operator growth, which are captured by the behavior of the Loschmidt echo and the average OTOC (i.e., the average operator size), respectively. For the former, we note that the Loschmidt echo fidelity with respect to a local operator is in fact equal to the *normalization* of the operator’s size distribution, $\mathcal{N}(t) = \langle \hat{M}(t) \hat{M}(t) \rangle = \int dSP(\mathcal{S})$. Our framework predicts [57] that the Loschmidt echo decays in time at a rate equal to the average size multiplied by the error rate:

$$\partial_t \log \mathcal{N}(t) = -2\varepsilon \bar{\mathcal{S}}(t). \quad (5)$$

Turning to the OTOC, we note that errors decrease the amplitude of large-size components of $\hat{M}(t)$ at a faster rate than small-size components. Thus, compared to purely unitary evolution, open-system dynamics inhibit the growth of operators. More specifically, we predict that the average size, $\bar{\mathcal{S}}$ [related to the OTOC via Eq. (2)], evolves according to

$$\partial_t \bar{\mathcal{S}}(t) = (\text{unitary}) - 2\varepsilon \delta \mathcal{S}(t)^2. \quad (6)$$

Here, the first term captures the specific unitary dynamics of the system, while the second term decreases the size at a rate proportional to the variance of the size distribution, $\delta \mathcal{S}^2$.

We now apply our framework to five paradigmatic classes of scrambling dynamics (Table I, Figs. 1–3): local and all-to-all interacting systems, local systems with conservation laws, long-range interacting systems, and free fermion integrable systems (see Supplemental Material for the latter two cases [44]). We begin by demonstrating that operator growth in the first two classes—systems with no conserved quantities under local and all-to-all interactions—are affected by open-system dynamics in drastically different ways.

For the former (focusing on 1D systems for specificity), one expects operators to grow ballistically in time under unitary dynamics, $\bar{\mathcal{S}} \approx \frac{3}{2} v_B t$, where v_B is the butterfly velocity. Meanwhile, the width of the operator’s size distribution grows “diffusively,” $\delta \mathcal{S} \approx c \sqrt{v_B t}$ where c is a constant [32,35,58]. Combining these expectations via

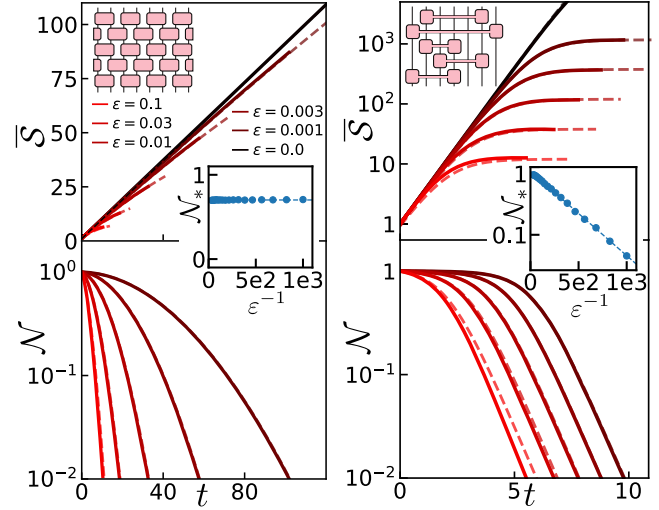


FIG. 2. (a) Average operator size, $\bar{\mathcal{S}}$, and the Loschmidt echo fidelity, \mathcal{N} , in a 1D RUC with $N = 200$ [44]. The size grows ballistically with quadratic corrections due to open-system dynamics (solid, data; dashed, theory). Inset: the Loschmidt echo fidelity, \mathcal{N}_* , when $(d\bar{\mathcal{S}}/dt) = 0.9(d\bar{\mathcal{S}}/dt)|_{\varepsilon=0}$, decays exponentially in the inverse error rate, ε^{-1} . (b) All-to-all RUC with $N = 1500$ [44]. The size grows exponentially before plateauing to a value which is independent of the system size. The decay rate of the Loschmidt echo is independent of ε after plateauing (solid, data; dashed, theory). Inset: the Loschmidt echo fidelity, \mathcal{N}_* , when $(d \log \bar{\mathcal{S}}/dt) = 0.9(d \log \bar{\mathcal{S}}/dt)|_{\varepsilon=0}$, is constant with respect to ε .

Eq. (6), we arrive at a simple phenomenological equation for operator growth under 1D *open-system* dynamics, $\lim_{x \rightarrow \infty} \partial_t \bar{\mathcal{S}} \approx \frac{3}{2} v_B - \varepsilon (c \sqrt{v_B t})^2$, whose solution yields the prediction: $\bar{\mathcal{S}}(t) \approx \frac{3}{2} v_B t - \frac{\varepsilon}{2} v_B t^2$. From Eq. (5), the Loschmidt echo fidelity thus decays as a Gaussian in time to leading order in ε , $\mathcal{N}(t) = \exp[-\varepsilon \int_0^t dt' \bar{\mathcal{S}}(t')] \approx \exp(-\frac{3}{4} \varepsilon v_B t^2)$.

To explore these predictions, we numerically simulate dynamics in a 1D random unitary circuit (RUC) [32,59] with single-qubit decoherence [44]. As shown in Fig. 2(a), we find that both the operator size and the Loschmidt echo fidelity (solid lines) agree remarkably well with our phenomenological predictions (dashed lines) across multiple orders of magnitude in the error rate.

In all-to-all interacting systems, unitary dynamics instead typically exhibit “fast scrambling” characterized by the exponential growth of operator size in time, $\bar{\mathcal{S}} \sim e^{\lambda t}$, where λ is the Lyapunov exponent [35,60–64]. Unlike local systems, the size distribution is also extremely broad, $\delta \mathcal{S} \approx b \bar{\mathcal{S}}$ where b is a constant, owing to the exponential growth of early-time fluctuations [33–35]. Solving Eq. (6), i.e., $\partial_t \bar{\mathcal{S}} \approx \lambda \bar{\mathcal{S}} - \varepsilon b^2 \bar{\mathcal{S}}^2$, then yields an intriguing prediction: under open-system dynamics, the average operator size *plateaus* to a system-size independent value, $\bar{\mathcal{S}}_p \approx \lambda / (\varepsilon b^2)$, after a time $t_p \sim \log[\lambda / (\varepsilon b^2)]$. This causes the Loschmidt echo to approach a constant rate of decay,

$\mathcal{N}(t) \sim \exp(-\lambda t/b^2)$. Notably, the decay rate, λ/b^2 , is *independent* of the microscopic error rate, ε , echoing seminal results in single-particle quantum chaos [55] and tantalizing recent NMR experiments [9–11]. As shown in Fig. 2(b), both of these predictions are indeed born out by RUC simulations.

One can further sharpen the distinction between open-system dynamics with local versus all-to-all interactions by analyzing their behavior at asymptotically small error rates. Specifically, consider the value of the Loschmidt echo, \mathcal{N}_* , at a time when the open-system dynamics have substantially deviated from the unitary dynamics. In all-to-all systems, this occurs shortly after the plateau time, t_p , which gives an order one Loschmidt echo, $\mathcal{N}(t_p) \approx \exp(-\varepsilon \int_0^{t_p} dt' e^{\lambda t'}) \approx \exp(-1/b^2)$, independent of the error rate [inset, Fig. 2(b)]. In contrast, in 1D, the influence of open-system dynamics on operator growth becomes substantial only once $(\varepsilon v_B t^2 / v_B t) \sim 1$, at which time the Loschmidt echo has decayed to an *exponentially* small value, $\mathcal{N}(t) \sim \exp(-v_B/\varepsilon)$ [inset, Fig. 2(a)]. For small error rates, this implies that large deviations in operator growth are in practice unobservable for local systems, since the signal is exponentially small in $1/\varepsilon$. Physically, this is a direct consequence of the asymptotic separation, $\delta S \ll \bar{S}$.

Effects of conservation laws.—We now show that the above behaviors are strikingly modified when an operator has overlap with a conserved quantity, $\hat{Q} = \sum_i \hat{q}_i$ (e.g., the total spin, or the Hamiltonian). Such systems feature an interplay between hydrodynamics and scrambling, which is embodied by a “bimodal” profile for unitary time-evolved operators [65,66]:

$$\hat{M}(t) = \sum_i q(i, t) \hat{q}_i + \sum_{\hat{R} \neq \hat{q}_i} c_R(t) \hat{R}. \quad (7)$$

The operator contains both small-size components, \hat{q}_i , representing the dynamics of the conserved quantity, as well as large-size Pauli strings, \hat{R} , representing scrambled information.

The small-size components arise because an operator’s overlap with \hat{Q} , $\langle \hat{M}(t) \hat{Q} \rangle = \sum_i q(i, t)$, is conserved in time. As an example, in ergodic 1D systems, one expects the local overlap, $q(i, t) = \langle \hat{M}(t) \hat{q}_i \rangle$, to spread diffusively, which causes the total normalization of the small-size components to decay in time, $\sum_i |q(i, t)|^2 \sim 1/\sqrt{t}$. This in turn implies that the total normalization of the large-size Pauli strings is increasing in time; physically, this corresponds to the dynamics of $q(i, t)$ “emitting” chaotic components, which spread ballistically from thereon. In combination, this leads to a size distribution (Fig. 1), $P(S) \approx (1/\sqrt{Dt}) \delta_{S, S_{q_i}} + (v_B/\sqrt{D}) (\frac{3}{2} v_B t - S)^{-3/2}$, where S_{q_i} is the size of the hydrodynamic components [67].

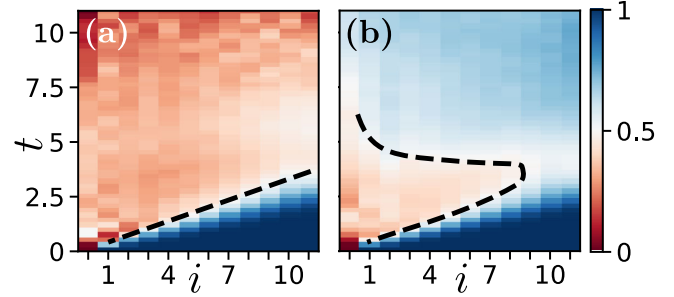


FIG. 3. OTOC as a function of time and space for an $N = 12$ one-dimensional spin chain. (a) Operators that do not overlap the Hamiltonian exhibit an OTOC which follows a ballistic light cone. (b) For an operator that overlaps with the Hamiltonian, the OTOC at a given site i initially decays, before increasing at later times. To demonstrate the generality of our framework, we calculate the OTOC in the perturbed Hamiltonian scenario, $\frac{1}{4} \sum_P \langle e^{-iH_1 t} \hat{M} e^{iH_1 t} \hat{P}_i e^{-iH_2 t} \hat{M} e^{iH_2 t} \hat{P}_i \rangle / \mathcal{N}(t)$, where the forwards and backwards time evolution are governed by two distinct 1D Hamiltonians, $H_1 = H_2 + \eta \delta H$ (for details see Supplemental Material [44]).

We expect open-system dynamics to damp the large-size components of \hat{M} by a factor $\sim e^{-\varepsilon S^2 / v_B}$, where S^2 / v_B is the space-time volume of the components’ light cone [68]. This effectively truncates the size distribution above $S_{tr} \sim \sqrt{v_B / \varepsilon}$ (Fig. 1). This suggests that the average operator size will actually *shrink* in time once $v_B t \gtrsim S_{tr}$, since small-size components decay more slowly, $P(S_{q_i}) \sim t^{-1/2}$, than large-size components, $P(S_{tr}) \sim t^{-3/2}$. This sharply contrasts with the behavior of operators that do not overlap conserved quantities, where one expects monotonic growth [Fig. 2(a)].

To explore this, we simulate the dynamics of a one-dimensional spin chain with generic interactions and measure the OTOC as a proxy for operator growth [44]. For an operator that does not overlap with the Hamiltonian, we find that the OTOC decays monotonically following a linear light cone [Fig. 3(a)]. For an operator exhibiting overlap, we find that the decay of the OTOC indeed *reverses* as a function of time, indicative of a decrease in the average operator size [Fig. 3(b)]. Interestingly, this insight immediately resolves an apparent disagreement between previous studies of open-system operator growth. In particular, certain studies found that OTOCs were only minimally affected by errors [13,24], while others found a dramatic reversal of scrambling [23,25]. We attribute this difference to the presence or absence of conservation laws.

Experimental implications.—Our results lead to a number of implications. First, we provide a new perspective on protocols which divide error-prone OTOC measurements by an independent characterization of the error [9,13,23,24]. In our language, the latter is precisely the normalization, $\mathcal{N}(t) = \langle \hat{M}(t) \hat{M}(t) \rangle$. To this end, these

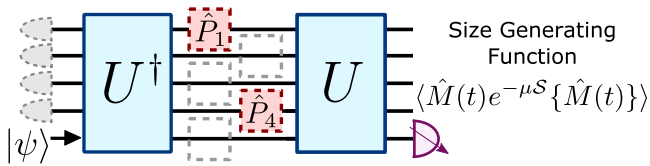


FIG. 4. Protocol to measure the generating function, $G_S(\mu)$, of the operator’s size distribution. Gray qubits are initially random in the computational basis, $|\psi\rangle$ is an \hat{M} eigenstate, and each site is acted upon randomly by either the identity (gray) or a nonidentity Pauli operator (red) in each experimental shot.

protocols will only replicate unitary dynamics when the total error is small ($1 - \mathcal{N} \approx \epsilon \int_0^t dt \bar{\mathcal{S}} \ll 1$) or when size distributions are tightly peaked, $\delta\mathcal{S} \ll \bar{\mathcal{S}}$.

Second, our results suggest a novel protocol for measuring operator size distributions (Fig. 4), which circumvents the need to either perform exponentially many measurements [69] or utilize two entangled copies of the system [35]. Specifically, in order to measure the *generating function* of the size distribution, $G_S(\mu) = \sum_{\mathcal{S}} P(\mathcal{S}) e^{-\mu\mathcal{S}}$, we propose the following protocol (Fig. 4): (i) prepare an initial state, $\rho = (1 + \hat{M}) \otimes \mathbb{1}^{\otimes N-1}/2^N$, (ii) time-evolve forward, e.g., via a unitary operation, U , (iii) apply a set of single-qubit Pauli operators, $\{\hat{P}_1, \dots, \hat{P}_N\}$, (iv) time-evolve backward via U^\dagger , and (v) measure \hat{M} . If the intervening Pauli operators are fixed, this reduces to previous schemes for measuring OTOCs [8]. However, if one randomly samples each Pauli matrix in each experimental shot, with probability $p = (1 - e^{-\mu})/4$ to be $\{\hat{X}, \hat{Y}, \hat{Z}\}$ and probability $1 - 3p$ to be the identity, this in effect implements a decoherence channel, $e^{-\mu\mathcal{S}}$, that explicitly depends on the size superoperator. The fidelity to recover the initial state then gives the generating function via $\mathcal{F} = \frac{1}{2}[1 + \mathcal{N}G_S(\mu)]$, where \mathcal{N} can be measured by setting $\mu = 0$.

Finally, we conjecture that our framework provides a theoretical underpinning to NMR experiments on the Loschmidt echo in the perturbed Hamiltonian scenario [9–11,70]. Indeed, recent experiments observe precisely our predicted linear scaling of the Loschmidt echo decay rate with the average operator size [11]. Somewhat intriguingly, this transitions to a square root scaling at small η ; developing a microscopic understanding of this regime remains an open question. Our protocol to measure size distributions also suggests a resolution to another open question in NMR experiments, regarding non-Gaussianities in “spin counting” protocols [9–11,71,72]. Namely, these non-Gaussianities detect higher moments of the operator’s size distribution [73].

Looking forward, our results also have implications for the classical simulability of open quantum systems—if operator sizes are bounded from above by a constant, \mathcal{S}_e , then time evolution is in principle efficiently simulable,

since the dimension of the accessible operator space is polynomial in the system size, $\sim N^{\mathcal{S}_e}$. A similar idea was recently proposed in diffusive 1D spin chains [67]; our results suggest that it may hold more broadly.

We are grateful to E. Altman, A. Kulkarni, R. Sahay, and M. Zalatel for illuminating discussions and to B. Kobrin and F. Machado for detailed feedback on the manuscript. This work is supported by the U.S. Department of Energy through the Quantum Information Science Enabled Discovery (QuantISED) for High Energy Physics (KA2401032) and through the GeoFlow Grant No. de-sc0019380. N. Y. Y. acknowledges support from the David and Lucile Packard foundation and a Simons Investigator award.

- [1] A. Bohrdt, C. B. Mendl, M. Endres, and M. Knap, *New J. Phys.* **19**, 063001 (2017).
- [2] F. Verstraete, J. J. Garcia-Ripoll, and J. I. Cirac, *Phys. Rev. Lett.* **93**, 207204 (2004).
- [3] D. Harlow, *Rev. Mod. Phys.* **88**, 015002 (2016).
- [4] E. H. Lieb and D. W. Robinson, in *Statistical Mechanics* (Springer, New York, 1972), pp. 425–431.
- [5] D. A. Roberts, D. Stanford, and L. Susskind, *J. High Energy Phys.* **03** (2015) 051.
- [6] D. E. Parker, X. Cao, A. Avdoshkin, T. Scaffidi, and E. Altman, *Phys. Rev. X* **9**, 041017 (2019).
- [7] J. Li, R. Fan, H. Wang, B. Ye, B. Zeng, H. Zhai, X. Peng, and J. Du, *Phys. Rev. X* **7**, 031011 (2017).
- [8] M. Gärtner, J. G. Bohnet, A. Safavi-Naini, M. L. Wall, J. J. Bollinger, and A. M. Rey, *Nat. Phys.* **13**, 781 (2017).
- [9] C. M. Sánchez, A. K. Chattah, K. X. Wei, L. Buljubasich, P. Cappellaro, and H. M. Pastawski, *Phys. Rev. Lett.* **124**, 030601 (2020).
- [10] C. M. Sánchez, A. K. Chattah, and H. M. Pastawski, *Phys. Rev. A* **105**, 052232 (2022).
- [11] F. D. Domínguez, M. C. Rodríguez, R. Kaiser, D. Suter, and G. A. Álvarez, *Phys. Rev. A* **104**, 012402 (2021).
- [12] F. D. Domínguez and G. A. Álvarez, *Phys. Rev. A* **104**, 062406 (2021).
- [13] X. Mi, P. Roushan, C. Quintana, S. Mandra, J. Marshall, C. Neill, F. Arute, K. Arya, J. Atalaya, R. Babbush *et al.*, *Science* **374**, 1479 (2021).
- [14] J. Cotler, T. Schuster, and M. Mohseni, [arXiv:2208.02256](https://arxiv.org/abs/2208.02256).
- [15] R. Islam, R. Ma, P. M. Preiss, M. E. Tai, A. Lukin, M. Rispoli, and M. Greiner, *Nature (London)* **528**, 77 (2015).
- [16] K. A. Landsman, C. Figgatt, T. Schuster, N. M. Linke, B. Yoshida, N. Y. Yao, and C. Monroe, *Nature (London)* **567**, 61 (2019).
- [17] M. S. Blok, V. V. Ramasesh, T. Schuster, K. O’Brien, J.-M. Kreikebaum, D. Dahlen, A. Morvan, B. Yoshida, N. Y. Yao, and I. Siddiqi, *Phys. Rev. X* **11**, 021010 (2021).
- [18] T. Brydges, A. Elben, P. Jurcevic, B. Vermersch, C. Maier, B. P. Lanyon, P. Zoller, R. Blatt, and C. F. Roos, *Science* **364**, 260 (2019).
- [19] M. K. Joshi, A. Elben, B. Vermersch, T. Brydges, C. Maier, P. Zoller, R. Blatt, and C. F. Roos, *Phys. Rev. Lett.* **124**, 240505 (2020).

- [20] F. Arute, K. Arya, R. Babbush, D. Bacon, J. C. Bardin, R. Barends, R. Biswas, S. Boixo, F. G. Brandao, D. A. Buell *et al.*, *Nature (London)* **574**, 505 (2019).
- [21] J. R. G. Alonso, N. Y. Halpern, and J. Dressel, *Phys. Rev. Lett.* **122**, 040404 (2019).
- [22] B. Yoshida and N. Y. Yao, *Phys. Rev. X* **9**, 011006 (2019).
- [23] B. Swingle and N. Y. Halpern, *Phys. Rev. A* **97**, 062113 (2018).
- [24] B. Vermersch, A. Elben, L. M. Sieberer, N. Y. Yao, and P. Zoller, *Phys. Rev. X* **9**, 021061 (2019).
- [25] Y.-L. Zhang, Y. Huang, and X. Chen *et al.*, *Phys. Rev. B* **99**, 014303 (2019).
- [26] K. Agarwal and N. Bao, *Phys. Rev. D* **102**, 086017 (2020).
- [27] N. Bao and Y. Kikuchi, *J. High Energy Phys.* **02** (2021) 017.
- [28] A. Touil and S. Deffner, *PRX Quantum* **2**, 010306 (2021).
- [29] F. Andreadakis, N. Anand, and P. Zanardi, *Phys. Rev. A* **107**, 042217 (2023).
- [30] J. Harris, B. Yan, and N. A. Sinitsyn, *Phys. Rev. Lett.* **129**, 050602 (2022).
- [31] A. Bhattacharya, P. Nandy, P. P. Nath, and H. Sahu, *J. High Energy Phys.* **12** (2022) 081.
- [32] A. Nahum, S. Vijay, and J. Haah, *Phys. Rev. X* **8**, 021014 (2018).
- [33] D. A. Roberts, D. Stanford, and A. Streicher, *J. High Energy Phys.* (2018) 122.
- [34] X.-L. Qi and A. Streicher, *J. High Energy Phys.* **08** (2019) 012.
- [35] T. Schuster, B. Kobrin, P. Gao, I. Cong, E. T. Khabiboulline, N. M. Linke, M. D. Lukin, C. Monroe, B. Yoshida, and N. Y. Yao, *Phys. Rev. X* **12**, 031013 (2022).
- [36] J. Loschmidt, *Kais. Akad. Wiss. Wien, Math. Naturwiss* **73**, 128 (1876).
- [37] A. Goussev, R. A. Jalabert, H. M. Pastawski, and D. Wisniacki, *Scholarpedia* **7**, 11687 (2012).
- [38] B. Yan, L. Cincio, and W. H. Zurek, *Phys. Rev. Lett.* **124**, 160603 (2020).
- [39] A. Larkin and Y. N. Ovchinnikov, *Sov. Phys. JETP* **28**, 1200 (1969).
- [40] S. Xu and B. Swingle, [arXiv:2202.07060](https://arxiv.org/abs/2202.07060).
- [41] This behavior has been noted qualitatively in previous works [11,25,42] and quantitatively in the context of random circuits [13]. It is familiar from, for example, quantum sensing, where many-body correlations in the GHZ state, $|\text{GHZ}\rangle = (|0^{\otimes n}\rangle + |1^{\otimes n}\rangle)/\sqrt{2}$, lead both to an increased sensitivity to magnetic fields as well as to increased dephasing [43].
- [42] C. M. Sánchez, R. H. Acosta, P. R. Levstein, H. M. Pastawski, and A. K. Chattah, *Phys. Rev. A* **90**, 042122 (2014).
- [43] C. L. Degen, F. Reinhard, and P. Cappellaro, *Rev. Mod. Phys.* **89**, 035002 (2017).
- [44] See Supplemental Material at <http://link.aps.org/supplemental/10.1103/PhysRevLett.131.160402>, which also contains Refs. [45–53], for additional details.
- [45] B. Yoshida and A. Kitaev, [arXiv:1710.03363](https://arxiv.org/abs/1710.03363).
- [46] D. A. Roberts and B. Yoshida, *J. High Energy Phys.* **04** (2017) 121.
- [47] S. Xu and B. Swingle, *Nat. Phys.* **16**, 199 (2020).
- [48] X. Chen and T. Zhou, *Phys. Rev. B* **100**, 064305 (2019).
- [49] T. Zhou, S. Xu, X. Chen, A. Guo, and B. Swingle, *Phys. Rev. Lett.* **124**, 180601 (2020).
- [50] O. Hallatschek and D. S. Fisher, *Proc. Natl. Acad. Sci. U.S.A.* **111**, E4911 (2014).
- [51] S. Chatterjee and P. S. Dey, *Commun. Pure Appl. Math.* **69**, 203 (2016).
- [52] D. Gottesman, [arXiv:quant-ph/9807006](https://arxiv.org/abs/quant-ph/9807006).
- [53] C. Dankert, R. Cleve, J. Emerson, and E. Livine, *Phys. Rev. A* **80**, 012304 (2009).
- [54] Note that our original use of the term Loschmidt echo refers to the case where one evolves forwards and backwards with the same Hamiltonian in the presence of noise and errors. The term Loschmidt echo is also used to describe the scenario here, where one evolves forwards and backwards with two different Hamiltonians.
- [55] R. A. Jalabert and H. M. Pastawski, *Phys. Rev. Lett.* **86**, 2490 (2001).
- [56] F. M. Cucchietti, D. A. R. Dalvit, J. P. Paz, and W. H. Zurek, *Phys. Rev. Lett.* **91**, 210403 (2003).
- [57] We derive Eqs. (5) and (6) by differentiating \mathcal{N} and $\bar{\mathcal{S}}$ with respect to t and applying Eq. (4).
- [58] C. W. Von Keyserlingk, T. Rakovszky, F. Pollmann, and S. L. Sondhi, *Phys. Rev. X* **8**, 021013 (2018).
- [59] A. Nahum, J. Ruhman, S. Vijay, and J. Haah, *Phys. Rev. X* **7**, 031016 (2017).
- [60] S. Sachdev and J. Ye, *Phys. Rev. Lett.* **70**, 3339 (1993).
- [61] A. Kitaev, A simple model of quantum holography, in KITP strings seminar and Entanglement 2015 program (2015), <http://online.kitp.ucsb.edu/online/entangled15/>.
- [62] J. Maldacena and D. Stanford, *Phys. Rev. D* **94**, 106002 (2016).
- [63] B. Kobrin, Z. Yang, G. D. Kahanamoku-Meyer, C. T. Olund, J. E. Moore, D. Stanford, and N. Y. Yao, *Phys. Rev. Lett.* **126**, 030602 (2021).
- [64] G. Bentsen, Y. Gu, and A. Lucas, *Proc. Natl. Acad. Sci. U.S.A.* **116**, 6689 (2019).
- [65] V. Khemani, A. Vishwanath, and D. A. Huse, *Phys. Rev. X* **8**, 031057 (2018).
- [66] T. Rakovszky, F. Pollmann, and C. W. Von Keyserlingk, *Phys. Rev. X* **8**, 031058 (2018).
- [67] T. Rakovszky, C. von Keyserlingk, and F. Pollmann, *Phys. Rev. B* **105**, 075131 (2022).
- [68] In systems with conserved quantities, the large-size Pauli strings also feature a heterogeneous structure, in which Pauli strings are more likely to commute with the conserved quantity near the wavefront of operator spreading, and only approach fully random behavior in the interior [65,66]. In principle, this implies that the wavefront is less susceptible to errors that preserve the conserved quantity.
- [69] X.-L. Qi, E. J. Davis, A. Periwal, and M. Schleier-Smith, [arXiv:1906.00524](https://arxiv.org/abs/1906.00524).
- [70] J. Baum and A. Pines, *Physica (Amsterdam)* **283A**, 166 (2000).
- [71] J. Baum, M. Munowitz, A. N. Garroway, and A. Pines, *J. Chem. Phys.* **83**, 2015 (1985).
- [72] J. Baum and A. Pines, *J. Am. Chem. Soc.* **108**, 7447 (1986).
- [73] The protocols discussed involve an intermediate global spin rotation by an angle φ . By arguments similar to those in the main text, we expect that this can be approximated as a decohering channel of strength $\mu \sim \varphi^2$ when acted on operators time evolved under ergodic many-body dynamics. We postpone a full investigation and discussion to future work.